

Reversibly tunable plasmonic bandgap by responsive hydrogel grating

Nityanand Sharma,^{1,2} Christian Petri,^{1,3} Ulrich Jonas,^{3,4} and Jakub Dostalek^{1,*}

¹AIT - Austrian Institute of Technology, Biosensor Technologies, Muthgasse 11, 1190 Vienna, Austria

²Nanyang Technological University, Centre for Biomimetic Sensor Science, 637553, Singapore

³Macromolecular Chemistry, University of Siegen, Department Chemistry-Biology, Adolf-Reichwein-Strasse 2, Siegen 57076, Germany

⁴Foundation for Research and Technology Hellas (FORTH), P.O. Box 1527, 71110 Heraklion, Crete, Greece

*jakub.dostalek@ait.ac.at

Abstract: Reversible actuating of surface plasmon propagation by responsive hydrogel grating is reported. Thermo-responsive poly(*N*-isopropylacrylamide)-based (pNIPAAm) hydrogel nanostructure was designed and tethered to a gold surface in order to switch on and off Bragg scattering of surface plasmons which is associated with an occurrence of a bandgap in their dispersion relation. pNIPAAm-based grating with a period around 280 nm was prepared by using photo-crosslinkable terpolymer and laser interference lithography and it was brought in contact with water. The temperature induced swelling and collapse of pNIPAAm hydrogel grating strongly modulates its refractive index ($\Delta n \sim 0.1$) which leads to the reversible opening and closing of a plasmonic bandgap. The experiments demonstrate partial opening of a bandgap with the width of 12 nm at wavelength around 800 nm where SPR exhibited the spectral width of about 75 nm.

©2016 Optical Society of America

OCIS codes: (240.6680) Surface plasmons; (250.5403) Plasmonics; (050.0050) Diffraction and gratings; (160.5470) Polymers.

References and links

1. J. Homola, "Surface plasmon resonance sensors for detection of chemical and biological species," *Chem. Rev.* **108**(2), 462–493 (2008).
2. K. R. Catchpole and A. Polman, "Plasmonic solar cells," *Opt. Express* **16**(26), 21793–21800 (2008).
3. J. R. Krenn, H. Ditlbacher, G. Schider, A. Hohenau, A. Leitner, and F. R. Aussenegg, "Surface plasmon micro- and nano-optics," *J. Microsc.* **209**(3), 167–172 (2003).
4. B. Schwarz, P. Reininger, D. Ristanić, H. Detz, A. M. Andrews, W. Schrenk, and G. Strasser, "Monolithically integrated mid-infrared lab-on-a-chip using plasmonics and quantum cascade structures," *Nat. Commun.* **5**, 4085 (2014).
5. J. Lin, J. P. Mueller, Q. Wang, G. Yuan, N. Antoniou, X. C. Yuan, and F. Capasso, "Polarization-controlled tunable directional coupling of surface plasmon polaritons," *Science* **340**(6130), 331–334 (2013).
6. L. Li, T. Li, S. Wang, S. Zhu, and X. Zhang, "Broad band focusing and demultiplexing of in-plane propagating surface plasmons," *Nano Lett.* **11**(10), 4357–4361 (2011).
7. H. Ditlbacher, J. R. Krenn, N. Féridj, B. Lamprecht, G. Schider, M. Salerno, A. Leitner, and F. R. Aussenegg, "Fluorescence imaging of surface plasmon fields," *Appl. Phys. Lett.* **80**(3), 404–406 (2002).
8. M. U. González, J. C. Weeber, A. L. Baudrion, A. Dereux, A. L. Stepanov, J. R. Krenn, E. Devaux, and T. W. Ebbesen, "Design, near-field characterization, and modeling of 45 deg surface-plasmon Bragg mirrors," *Phys. Rev. B* **73**(15), 155416 (2006).
9. L. Yin, V. K. Vlasko-Vlasov, J. Pearson, J. M. Hiller, J. Hua, U. Welp, D. E. Brown, and C. W. Kimball, "Subwavelength focusing and guiding of surface plasmons," *Nano Lett.* **5**(7), 1399–1402 (2005).
10. W. L. Barnes, T. W. Preist, S. C. Kitson, and J. R. Sambles, "Physical origin of photonic energy gaps in the propagation of surface plasmons on gratings," *Phys. Rev. B Condens. Matter* **54**(9), 6227–6244 (1996).
11. W. L. Barnes, T. W. Preist, S. C. Kitson, J. R. Sambles, N. P. Cotter, and D. J. Nash, "Photonic gaps in the dispersion of surface plasmons on gratings," *Phys. Rev. B Condens. Matter* **51**(16), 11164–11167 (1995).
12. S. C. Kitson, W. L. Barnes, and J. R. Sambles, "Surface-plasmon energy gaps and photoluminescence," *Phys. Rev. B Condens. Matter* **52**(15), 11441–11445 (1995).

13. M. Toma, K. Toma, P. Adam, J. Homola, W. Knoll, and J. Dostálek, "Surface plasmon-coupled emission on plasmonic Bragg gratings," *Opt. Express* **20**(13), 14042–14053 (2012).
14. D. Kuckling, M. E. Harmon, and C. W. Frank, "Photo-cross-linkable PNIPAAm copolymers. I. Synthesis and characterization of constrained temperature-responsive hydrogel layers," *Macromol.* **35**(16), 6377–6383 (2002).
15. J. Gosciniaik, S. I. Bozhevolnyi, T. B. Andersen, V. S. Volkov, J. Kjelstrup-Hansen, L. Markey, and A. Dereux, "Thermo-optic control of dielectric-loaded plasmonic waveguide components," *Opt. Express* **18**(2), 1207–1216 (2010).
16. N. Zhang and W. Knoll, "Thermally responsive hydrogel films studied by surface plasmon diffraction," *Anal. Chem.* **81**(7), 2611–2617 (2009).
17. X. Dong, X. B. Zou, X. Y. Liu, P. Lu, J. M. Yang, D. L. Lin, L. Zhang, and L. S. Zha, "Temperature-tunable plasmonic property and SERS activity of the monodisperse thermo-responsive composite microgels with core-shell structure based on gold nanorod as core," *Colloid Surf. A* **452**, 46–50 (2014).
18. H. Gehan, C. Mangeney, J. Aubard, G. Lévi, A. Hohenau, J. R. Krenn, E. Lacaze, and N. Félidj, "Design and optical properties of active polymer-coated plasmonic nanostructures," *J. Phys. Chem. Lett.* **2**(8), 926–931 (2011).
19. M. Nguyen, X. Sun, E. Lacaze, P. M. Winkler, A. Hohenau, J. R. Krenn, C. Bourdillon, A. Lamouri, J. Grand, G. Lévi, L. Boubekeur-Lecaque, C. Mangeney, and N. Félidj, "Engineering thermoswitchable lithographic hybrid gold nanorods as plasmonic devices for sensing and active plasmonics applications," *ACS Photonics* **2**(8), 1199–1208 (2015).
20. P. W. Beines, I. Klosterkamp, B. Menges, U. Jonas, and W. Knoll, "Responsive thin hydrogel layers from photo-cross-linkable poly(*N*-isopropylacrylamide) terpolymers," *Langmuir* **23**(4), 2231–2238 (2007).
21. E. D. Palik, *Handbook of Optical Constants of Solids* (Academic Press, 1998).
22. M. Toma, U. Jonas, A. Mateescu, W. Knoll, and J. Dostálek, "Active control of SPR by thermo-responsive hydrogels for biosensor applications," *J Phys Chem C Nanomater Interfaces* **117**(22), 11705–11712 (2013).
23. M. J. Junk, R. Berger, and U. Jonas, "Atomic force spectroscopy of thermoresponsive photo-cross-linked hydrogel films," *Langmuir* **26**(10), 7262–7269 (2010).
24. A. Suzuki, M. Yamazaki, Y. Kobiki, and H. Suzuki, "Surface domains and roughness of polymer gels observed by atomic force microscopy," *Macromolecules* **30**(8), 2350–2354 (1997).
25. M. Guvendiren, S. Yang, and J. A. Burdick, "Swelling-induced surface patterns in hydrogels with gradient crosslinking density," *Adv. Funct. Mater.* **19**(19), 3038–3045 (2009).
26. S. Yang, K. Khare, and P. C. Lin, "Harnessing surface wrinkle patterns in soft matter," *Adv. Funct. Mater.* **20**(16), 2550–2564 (2010).
27. J. R. Lakowicz, K. Ray, M. Chowdhury, H. Szmecinski, Y. Fu, J. Zhang, and K. Nowaczyk, "Plasmon-controlled fluorescence: a new paradigm in fluorescence spectroscopy," *Analyst (Lond.)* **133**(10), 1308–1346 (2008).

1. Introduction

Surface plasmon polaritons (SPPs) are optical waves that originate from collective oscillations of charge density and associated electromagnetic field at a metallic surface. Optical excitation of these modes allows for tight confinement of light energy at the surface which is associated with enhanced field strength. These phenomena found numerous applications in areas ranging from detection and interaction analysis of biomolecules [1], light harvesting in thin film optical devices [2], to highly integrated optical circuits [3, 4]. In order to control propagation of SPPs on a 2D metallic surface, elements such as directional couplers [5], lens [6], splitters [7], and mirrors [8, 9] were developed. These elements can be designed in the form of periodic gratings on a metallic surface and utilize diffractive coupling of counter propagating SPPs which induces a plasmonic bandgap [10, 11]. At wavelengths that coincide with the bandgap, SPPs cease to exist and at the edges of the bandgap new coupled SPP modes with long range and short range surface plasmon characteristics occurs. Such phenomena were of interest in studies where SPP-mediated local density of states alters emission properties of fluorescence emitters [12, 13] and they were shown to provide versatile means for focusing, reflecting and splitting of 2D SPP beams [3, 8]. Up to now, the majority of diffractive structures that allow for 2D control of SPP propagation are static and after they are prepared their characteristics are fixed. Thermo-responsive polymers offer attractive materials to prepare actively tunable diffractive structures. Among them, poly(*N*-isopropylacrylamide) (pNIPAAm) represents a prominent example of material that can "on demand" swell and collapse by variations of temperature around its lower critical solution temperature (LCST). Below the LCST, pNIPAAm exhibits a highly open, water-swollen structure while above the LCST it collapses with a release of bound water. The swelling-

collapsing strongly alters its refractive index and for the crosslinked pNIPAAm hydrogel networks it can reach values as high as $\Delta n = 0.1$ [14] which exceeds values reported for other polymers employed thermo-actuating of surface plasmons [15]. pNIPAAm gratings with periods of several μm were prepared by contact mask lithography and surface plasmon resonance (SPR) spectroscopy was employed as a tool to enhance measured diffraction signal [16]. Other types of plasmonic structures that benefit from pNIPAAm in form of a microgel [17] or thin brush [18,19] were reported for actuating of localized surface plasmons supported by metallic nanoparticles. This work reports on the preparation of dense and tunable pNIPAAm gratings on a gold surface for reversibly opening and closing the plasmonic bandgap. Large-area structures were prepared by using a photo-crosslinkable pNIPAAm-based terpolymer and UV laser interference lithography (LIL). The thermo-actuating of polymer gratings is investigated and their ability to actively tune the SPP dispersion relation is demonstrated.

2. Materials and methods

2.1. Preparation of structured pNIPAAm layer

BK7 glass substrate was coated with 1.1 nm thick chromium film and 47 nm thick gold layer by vacuum thermal evaporation. On the top of the gold surface, SU-8 polymer layer with a thickness of ~ 5 nm was spin-coated. A solution with SU-8 2000 (from Micro Resist Technology GmbH, Germany) diluted to 2 vol% by SU-8 thinner (from Micro Resist Technology GmbH, Germany) was spun at 5000 rpm for 60 s followed by drying in vacuum oven at 50 °C for 2 hrs. The thin SU-8 layer served as a linker for the subsequent attachment of nanostructured responsive pNIPAAm-based hydrogel film. Terpolymer ($M_w = \text{ca. } 4 \times 10^5 \text{ g mol}^{-1}$) composed of *N*-isopropylacrylamide, methacrylic acid, and 4-methacryloyloxy benzophenone with a ratio of 94:5:1 was synthesized as reported before [20]. This polymer was dissolved in ethanol at a concentration of 2 wt% and deposited on SU-8 surface by spin-coating. Spin rate of 2000 rpm was applied for 2 min and subsequently the polymer layer was dried overnight in a vacuum oven at 50 °C.

The periodic grating depicted in Fig. 1 was generated in the photo-crosslinkable pNIPAAm-based layer with an interference field of two spatially overlapping coherent light beams at a wavelength 325 nm by using Lloyd configuration. A beam emitted from a He-Cd laser (IK3031R-C, Kimmon, Japan) was expanded and coupled to Lloyd's mirror in order to yield the periodic surface topography over an area of several cm^2 . The angle between the interfering beams was adjusted between $\theta = 35.48$ deg and 21.17 deg which corresponds to the period of harmonically oscillating intensity of $\lambda = 280$ nm and 450 nm. In order to prepare crossed gratings, the interference field of two beams was twice recorded to the pNIPAAm film on a substrate that was oriented at 0 and 90 deg. Irradiation time was adjusted between $t = 20$ and 30 min in order to take into account different angles of incidence of interfering beams θ so the average dose was kept constant at 0.69 J cm^{-2} . In the areas with maximum interference field intensity, crosslinking of the polymer layer networks occurs via the benzophenone groups attached to the pNIPAAm polymer backbone. In the areas where the interference field intensity exhibits its minimum, weak polymer crosslinking occurs and after rinsing with ethanol and water it is washed out. The topography of the dried pNIPAAm grating was measured in air by using an atomic force microscope (AFM, Molecular Imaging PicoPlus) that was operated in tapping mode.

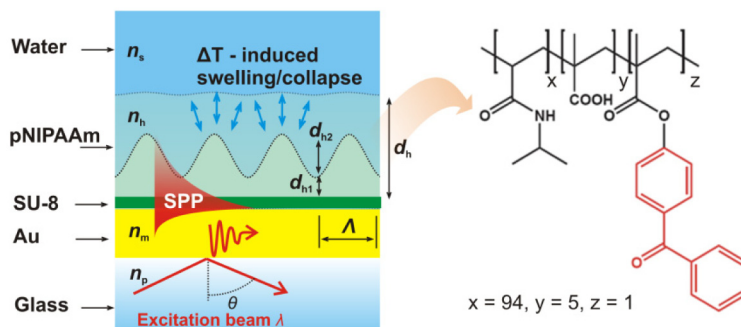


Fig. 1. a) Schematics of the prepared pNIPAAm-based grating that is probed by travelling SPP. b) Chemical structure of the photo-crosslinkable pNIPAAm terpolymer used in the interference lithography process.

2.2. Optical setup

An optical setup utilizing Kretschmann configuration of attenuated total reflection (ATR) method was employed to measure SPR reflectivity as a function of angle of incidence θ and wavelength λ . A polychromatic light emitted from a halogen lamp (LSH102 from LOT-Oriel, Germany) was coupled to an optical fiber M25L02 (Thorlabs, USA). The output light beam was collimated by an achromatic lens 14 KLA 001 CV1 (focal length $f = 60$ mm, Melles Griot, Germany), polarized by a rotational polarizer and launched into a 90° prism made from LASFN9 glass. A glass substrate with gold layer supporting SPPs and pNIPAAm grating on its top was optically matched to the prism base by using index matching immersion oil. The incident beam was totally internally reflected at the glass surface with gold layer. The angle of incidence θ was controlled by using a rotation stage (with precision of 0.005 deg from Huber GmbH, Germany) and the reflected beam was coupled via a lens F810SMA-635 (Thorlabs, USA) into a multimode optical fiber M26L02 (Thorlabs, USA) that was connected to a spectrometer HR4000 (Ocean Optics, USA). The reflectivity $R(\lambda, \theta)$ that was measured for transverse magnetic (TM) polarization was normalized with that obtained for transverse electric (TE) polarization. An in-house designed flow-cell with temperature control by Peltier device (connected to its driver LFI3751 from Wavelength Electronics, USA) was clamped against the coated glass substrate and water was pumped through by using a peristaltic pump with a tubing (ID 0.76, SC0008, IDEX Health & Science SA, Switzerland). The data acquisition and system control was performed by an in-house developed software tool developed in LabVIEW (National Instruments, USA).

2.3 Simulations

Simulations of diffraction coupling of counter-propagating SPPs by the hydrogel grating were performed numerically by using finite element method (FEM) that was implemented in a diffraction grating solver DiPoG (Weierstrass Institute, Germany). The refractive index of LASFN9 was assumed as $n_p = 1.845$ and that of water as $n_s = 1.33$. Refractive index of gold was assumed to be dispersive $n_m(\lambda)$ and it was taken from Palik [21]. Refractive index of SU-8 was set to 1.48 and the presence of chromium was omitted. The attached pNIPAAm hydrogel refractive index was $n_h = 1.36$ in the swollen state and $n_h = 1.48$ in the collapsed state. It should be noted that for simplicity the grating was assumed as being one dimensional (the surface was modulated only in one lateral direction that lied in the plane of incidence). The topographic profile was assumed to be sinusoidal with a period Λ and a modulation depth of d_{h2} . An additional residual hydrogel layer with a thickness d_{h1} in between the modulated zone and SU-8 was assumed. The refractive index inside the hydrogel was assumed to be homogeneous.

3. Results and discussion

Firstly, the swelling of a pNIPAAm layer that was not structured was measured by optical waveguide spectroscopy. In this experiment one of the UV interfering beams was blocked in order to crosslink the pNIPAAm layer homogeneously with a dose of 0.69 J cm^{-2} . After rinsing with water and drying, the thickness of the neat pNIPAAm layer was determined as $d_h \sim 72 \text{ nm}$ and the refractive index was $n_h = 1.48$ (data not shown). When the layer was swollen in contact with water at room temperature $T = 22 \text{ }^\circ\text{C}$, its thickness increased to $d_h \sim 370 \text{ nm}$ and the refractive index decreased to $n_h = 1.36$, which corresponds to a swelling ratio of about $SR \sim 5$. The reason for the refractive index decrease is the dilution of the polymer chain segment with water, which exhibits lower refractive index $n_s = 1.33$. When increasing the temperature, the pNIPAAm hydrogel layer collapsed at its LCST of $T = 32 \text{ }^\circ\text{C}$. At the temperature of $T = 37 \text{ }^\circ\text{C}$ the hydrogel layer exhibited thickness similar to that measured in the dry state $d_h \sim 69 \text{ nm}$ and a refractive index of $n_h = 1.48$. It should be noted that these observations on one-dimensional swelling constrained perpendicular to the layer surface are in accordance with our previous studies when an identical pNIPAAm film was crosslinked with a broad spectrum of non-coherent UV light centered at a wavelength of $\lambda = 365 \text{ nm}$ with a dose $5\text{-}20 \text{ J cm}^{-2}$ [22].

Afterwards, a series of pNIPAAm gratings with varying period of $\Lambda = 280 - 450 \text{ nm}$ were written by coherent and interfering UV beams with same average dose of 0.69 J cm^{-2} . After recording the sinusoidally modulated crosslinking density, the pNIPAAm layer was rinsed with water in order to remove any loosely bound polymer chains, in particular from areas that were exposed only to weak UV light intensity. In water at room temperature $T = 22 \text{ }^\circ\text{C}$, the polymer network swells and polymer chains rearrange. During subsequent drying of the pNIPAAm grating, the strong surface tension of the water-air interface deforms the elastic polymer network and leads to a planarization of the soft grating as it reaches the hydrogel layer during water evaporation. This is clearly visible in the completely flat surface in the AFM image of Fig. 2(a) for a hydrogel structure with a recorded periodicity of $\Lambda = 310 \text{ nm}$. Interestingly, when the same structure is swollen in water at a temperature $T = 22 \text{ }^\circ\text{C}$ and subsequently heated to a higher temperature above the LCST before drying, the written pattern is retained as shown in Fig. 2(b).

The behavior is explained by the substantial increase of the mechanical modulus in the hydrogel film above the transition temperature [23], which prevents its deformation by the surface tension when the water-air interface reaches the grating surface. At the higher temperature the polymer film collapses in contact with the aqueous medium to form a topographic structure resembling the original recorded cross-linked pattern. Afterwards, the water evaporates from the polymer film surface and the written crosslink density modulation can be observed as a relief grating.

As can be seen in Fig. 2(b), the relief grating with $\Lambda = 310 \text{ nm}$ exhibits indented features with a depth of about $d_{h2} = 80 \text{ nm}$ in air, but its periodic regularity is perturbed which can be attributed to the process of collapsing and drying. The deformation of planar, surface-attached hydrogel layers by swelling stresses was previously described in the literature [24, 25], which leads to the formation of buckling structures. In summary, the covalent grafting of the polymer network to the solid substrate confines the polymer network in the substrate plane and effectively allows expansion during swelling only in one dimension along the surface normal vector. Such confinement leads to the buildup of lateral swelling stress, which is released by undulation of the hydrogel layer surface in a buckling process and resulting in the characteristic crease topography. This effect is also expected to contribute to the distortion of the periodic nanostructures investigated here and may be more pronounced when the thickness in the swollen state d_h is comparable with the period Λ . Indeed, for a hydrogel hole array with much larger topographic dimensions and periodicities in the micrometer range, a transition of the circular hole geometry to a perpendicular diamond plate pattern was reported

upon swelling in water [26]. In order to investigate this swelling-collapse induced effect for sub-micron grating geometries, two gratings with same thickness d_h , but a shorter period of $\Lambda = 290$ nm and respectively a longer period $\Lambda = 450$ nm were examined. As seen in Fig. 2(c), the shorter period structure is significantly more perturbed than the longer period one in Fig. 2(d), which confirms that the ratio of thickness d_h and period Λ plays a crucial role in the swelling and collapsing of the highly open pNIPAAm network nanostructure.

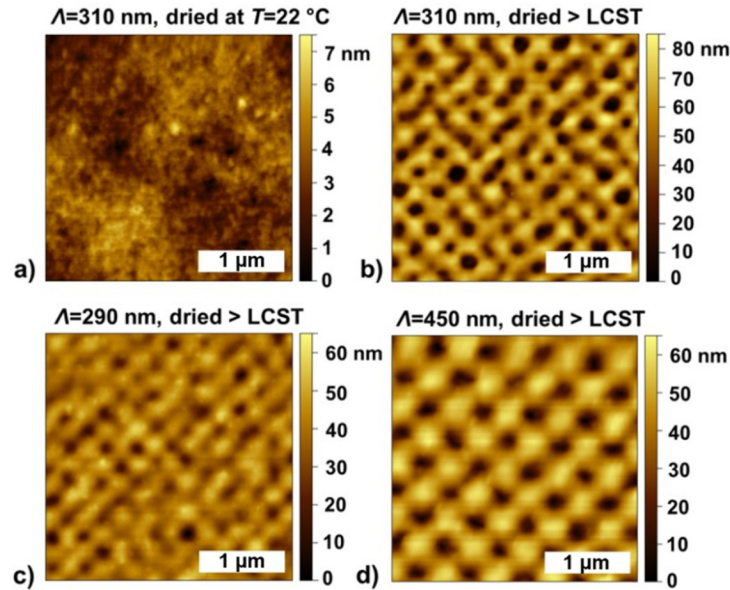


Fig. 2. AFM images of a pNIPAAm grating with $\Lambda = 310$ nm that was dried at a) room temperature $T = 22$ °C and b) at elevated temperature $T > \text{LCST}$. Comparison of the c) denser grating with $\Lambda = 290$ nm and sparser grating with $\Lambda = 450$ nm observed after drying at elevated temperature.

For the diffraction coupling of counter propagating SPPs on the Au surface, the period has to fulfill the following phase matching condition $2\text{Re}\{k_{\text{SPP}}\} = 2\pi/\Lambda$, where k_{SPP} is the (complex) propagation constant of SPPs. In order to induce the plasmonic bandgap at the wavelength around $\lambda \sim 800$ nm on a gold surface in contact with water, the period $\Lambda = 280$ nm was determined by a series of the following numerical simulations presented in Fig. 3.

As seen in Fig. 3(a), wavelength reflectivity spectra were simulated for the geometry representing the swollen and collapsed hydrogel grating. In the swollen state, a homogeneous layer with the thickness of $d_h = 372$ nm and refractive index $n_h = 1.36$ was assumed [Fig. 3(a)]. For the collapsed state, refractive index of the pNIPAAm of $n_h = 1.48$ was assumed and the outer interface with water was sinusoidally modulated [Fig. 3(a)-3(e)]. As summarized in the table presented in Fig. 3(f), the thickness of residual layer d_{h1} was adjusted for each modulation depth d_{h2} so the volume of the collapsed layer was kept fixed. The reflectivity curve in Fig. 3 (a) shows that for a swollen hydrogel film the coupling of incident light and the angle of incidence $\theta = 51.1$ deg is manifested as a resonant dip centered at $\lambda = 780$ nm. For the collapsed state of the polymer [curves in Fig. 3(a)-(e)], this resonance is split to two branches that become stronger separated when increasing the modulation depth d_{h2} . The reason for the splitting is the opening of a plasmonic bandgap due to Bragg scattering of the SPPs. This scattering leads to the cancellation of SPP propagation in a band centered at a wavelength $\lambda \sim 800$ nm, and when increasing the modulation depth d_{h2} the spectral width $\Delta\lambda$ is increasing. As the average refractive index probed by the SPPs for each geometry is slightly changing, the angle of incidence θ was adjusted for each configuration so the reflectivity

curve crosses through the middle of the gap and the minima associated to the lower wavelength SPP branch and higher wavelength SPP branch are the same. It is worth of noting that these two branches correspond to the ω^+ and ω^- modes at the edges of the plasmonic bandgap [11] with the field confined in the polymer or water. The reflectivity curves in Fig. 3(b)-(e) indicate that the collapsed linear hydrogel grating allows for opening a bandgap with the width $\Delta\lambda$ that approximately increases linearly with d_{h2} and can reach $\Delta\lambda = 28$ nm for the modulation depth $d_{h2} = 140$ nm of a linear grating.

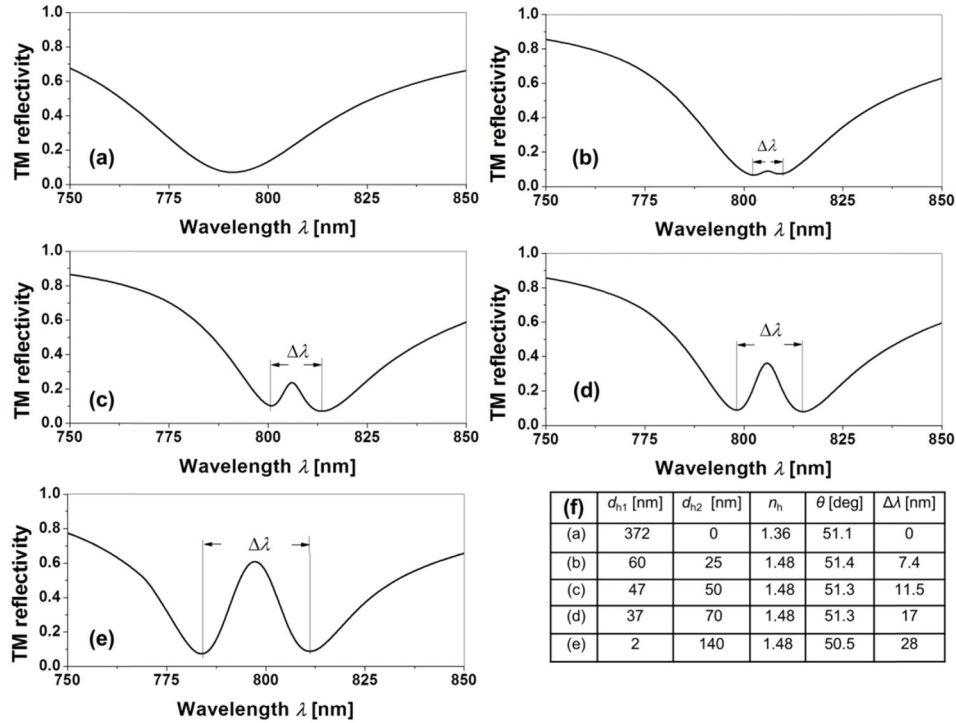


Fig. 3. Simulated wavelength reflectivity spectra for a flat swollen pNIPAAm film (a), and a series of combinations of modulation depth d_{h2} and residual layer thickness d_{h1} for a collapsed pNIPAAm film (b-e). Reflectivity spectra calculated for TM polarization were normalized with those simulated for TE polarization. f) Summary of structural parameters (defined in Fig. 1) used in the above simulations with the angle of incidence θ and plasmonic bandgap width $\Delta\lambda$.

The opening and closing of a plasmonic bandgap was experimentally observed on a pNIPAAm grating with a period of $\Lambda = 280$ nm. As seen in Fig. 4, there was measured reflectivity dependence on the angle of incidence θ and wavelength λ . These measurements were carried out at temperature $T = 22$ °C where the pNIPAAm structure swells in water [see Fig. 4(a)] and it was increased to $T = 34, 37, 45$ and 45 °C when it collapses. The resonant excitation of SPPs manifests itself as a dark band in the reflectivity spectrum which shifts to higher angles θ when decreasing the wavelength λ . At temperature above the pNIPAAm LCST ($T > 32$ °C) the average refractive index of the polymer layer probed by SPPs increases due to the collapsing of the pNIPAAm structure which is accompanied with the occurrence of SPR band at higher angles θ . In addition, the collapse of the pNIPAAm is associated with periodic modulating of refractive index. This grating induces splitting in the SPP dispersion relation due to the diffraction coupling of counter propagating SPPs on the surface as predicted by simulations in Fig. 3.

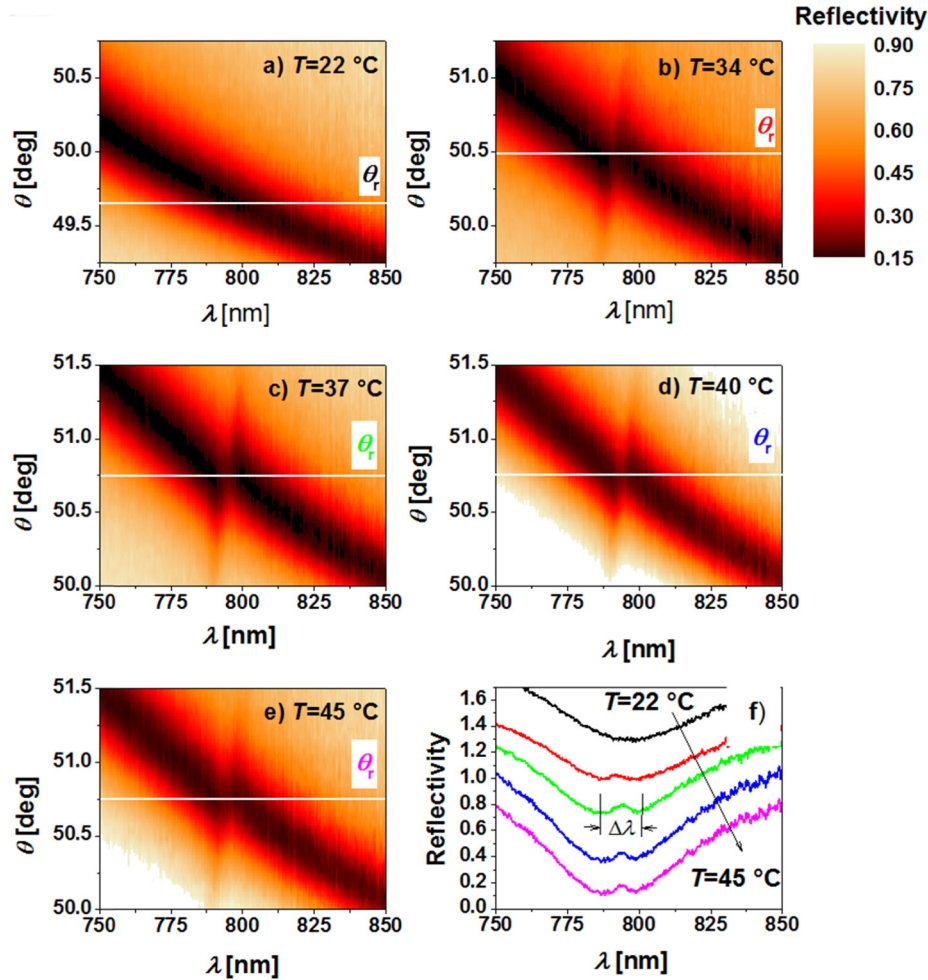


Fig. 4. Measured reflectivity dependence on θ and λ for a pNIPAAm grating with the period $\Lambda = 280$ nm and temperature a) $T = 22$ °C, b) $T = 34$ °C, c) $T = 37$ °C, d) $T = 40$ °C, and e) $T = 45$ °C. f) Cross-section of reflectivity at each temperature for the indicated angle of incidence θ_{res} at which the bandgap occurs for a pNIPAAm grating with the periodicity $\Lambda = 280$ nm. Subsequent reflectivity curves are offset by 0.3 along the reflectivity axis. Reflectivity spectra measured for TM polarization were normalized with those obtained for TE polarization in all graphs.

In order to evaluate the width of the bandgap, cross-sections of SPR reflectivity at θ_r indicated in Figs. 4(a)-4(e) were plotted in Fig. 4(f). These plots show that the gradual collapse of the grating leads to the opening of plasmonic bandgap. Interestingly, the width of the bandgap increases with temperature and reaches its maximum of $\Delta\lambda = 12$ nm at around $T = 37$ °C. It should be noted that measured bandgap width $\Delta\lambda$ is lower than the spectral width of SPR of 75 nm (determined as full width in the half minimum of reflectivity dip in Fig. 4(a)). Therefore, the full bandgap was not achieved and SPPs can partially propagate at the wavelength range between reflectivity minima. When further increasing the temperature to 40 and 45 °C, the bandgap width $\Delta\lambda$ slightly decreases which can be attributed to increasing hydrophobicity of the polymer and possible additional changes in the structure. When comparing the experimentally measured maximum bandgap width in Fig. 4 with simulations in Fig. 3, the modulation depth of pNIPAAm grating can be estimated as $d_{h2} \sim 50$ nm which is lower than values typically observed by AFM on prepared samples (see Fig. 2). This

discrepancy can be attributed to two following effects. Firstly, the grating observed *ex situ* in air exhibit probably more defects and flatter structure than that which is probed in water by SPPs. Secondly the experimental data were measured on a crossed grating and the simulations were (for simplicity) carried out for a linear grating. Therefore, the modulation depth used in experiments is effectively decreased by a factor of two by averaging in the direction perpendicular to SPP propagation.

4. Conclusions

In summary, we show that laser interference lithography can be used for the preparation of nanogratings from a photo-crosslinkable pNIPAAm-based polymer. These structures with periodically modulated crosslink density can be actuated in an aqueous medium by varying temperature, leading to swelling and collapsing of the structure, which is accompanied by a modulation of the refractive index contrast by about 0.1 in an on-or-off switch mode. A crossed grating structure with a period as small as 280 nm and modulation depth in the collapsed state of 60-80 nm was prepared and tested for opening and closing a plasmonic bandgap of the SPPs. The angular and wavelength spectroscopy of the surface plasmon polaritons demonstrated that the bandgap can be partially open with a width of about 12 nm for SPPs on the gold surface and at a wavelength of $\lambda \sim 800$ nm where SPR exhibited the spectral width of about 75 nm. In order to enlarge the spectral width of such a plasmonic bandgap the modulation depth of the structure can be further increased. Alternatively, the upper surface of the responsive polymer can be decorated with a flexible material that increases the refractive index contrast to the aqueous medium. We believe that this approach in conjunction with e.g. embedded ITO microheaters [22] may find its applications in 2D plasmonic optics and provide facile means to actively manipulate SPP beams and tune SPP dispersion relation. For instance the opening and closing of plasmonic bandgap by the presented hydrogel grating can provide means to actively control surface plasmon-coupled fluorescence emission [13]. For plasmonic biosensing with the surface plasmon-coupled emission readout [27], the presented responsive hydrogel can be modified with biomolecules [22] and directly utilized in assays for chemical and biological analytes present in aqueous environment.

Acknowledgments

This work was partially supported by Austrian Science Fund (FWF) through the project ACTIPLAS (P244920-N20) and Austrian Federal Ministry for Transport, Innovation and Technology (GZ BMVIT-612.166/0001-III/I1/2010) via the International Graduate School on Bionanotechnology, a joint Ph.D. program of the University of Natural Resources and Life Sciences Vienna (BOKU), the Austrian Institute of Technology (AIT), and the Nanyang Technological University (NTU). NS also acknowledges support from the School of Materials Science and Engineering and the provost's office, Nanyang Technological University, and JD support from Tan Chin Tuan foundation.